Infrared Physics & Technology 59 (2013) 22–27

Contents lists available at SciVerse ScienceDirect

Infrared Physics & Technology

journal homepage: www.elsevier.com/locate/infrared

Performance of mid-wave T2SL detectors with heterojunction barriers

Carl Asplund [a,*], Rickard Marcks von Würtemberg [a], Dan Lantz [a], Hedda Malm [a], Henk Martijn [a], Elena Plis [b], Nutan Gautam [b], Sanjay Krishna [b]

[a] IRnova AB, Electrum 236, S 164 40 Kista, Sweden
[b] Center for High Technology Materials, Department of Electrical and Computer Engineering, University of New Mexico, Albuquerque, NM 87106, USA

ARTICLE INFO

Article history:
Available online 19 January 2013

Keywords:
Infrared detectors
Strained layer superlattice
MWIR detectors
Focal plane array

ABSTRACT

A heterojunction T2SL barrier detector which effectively blocks majority carrier leakage over the pn-junction was designed and fabricated for the mid-wave infrared (MWIR) atmospheric transmission window. The layers in the barrier region comprised AlSb, GaSb and InAs, and the thicknesses were selected by using $k \cdot P$-based energy band modeling to achieve maximum valence band offset, while maintaining close to zero conduction band discontinuity in a way similar to the work of Abdollahi Pour et al. [1] The barrier-structure has a 50% cutoff at 4.75 μm and 40% quantum efficiency and shows a dark current density of 6×10^{-6} A/cm^2 at −0.05 V bias and 120 K. This is one order of magnitude lower than for comparable T2SL-structures without the barrier. Further improvement of the (non-surface related) bulk dark current can be expected with optimized doping of the absorber and barrier, and by fine tuning of the barrier layer design. We discuss the effect of barrier doping on dark current based on simulations. A T2SL focal plane array with 320 × 256 pixels, 30 μm pitch and 90% fill factor was processed in house using a conventional homojunction *p–i–n* photodiode architecture and the ISC9705 readout circuit. High-quality imaging up to 110 K was demonstrated with the substrate fully removed.

1. Introduction

High performance imaging infrared detectors operating in the 3–15 μm wavelength range are of interest for many applications within industry, as well as in surveillance and earth observation from space. Currently, high end IR detection systems are predominantly based on mercury cadmium telluride (MCT), indium antimonide (InSb), or quantum well infrared photodetector (QWIP) technologies. Recent progress in type-II InAs/GaSb based strained layer superlattice (T2SL) technology [2,3] has made it a promising candidate for high-performance infrared photodetection in the mid-wave (MWIR, 3–5 μm), as well as long-wave IR transmission band (LWIR, 8–12 μm and VLWIR, 11–15 μm). Among the advantages of T2SL is high quantum efficiency compared to QWIP; large electron effective mass, low Auger generation rate [4], and thickness dependent, rather than composition-dependent bandgap, which promises better spatial uniformity as compared to MCT. Present state-of-the-art T2SL detectors are, however, depletion current limited at temperatures up to approximately 140 K, with Shockley–Read–Hall (SRH) lifetimes of a few tens of ns. This lifetime is two orders of magnitude shorter than for MCT, so the strongly reduced Auger generation rate of T2SL cannot really be exploited until the defects responsible for the SRH process are identified and eliminated [5].

Since the space-charge SRH current, also called generation–recombination (G–R) current, is proportional to the intrinsic carrier concentration, $n_i \propto \exp(-E_g/2kT)$, where E_g is the bandgap, many ways have been proposed to increase the bandgap of the depletion region, while still allowing free passage for the photogenerated carriers. Among these are minority carrier unipolar concepts such as *n*Bn [7–9], *p*Bp [10], and heterojunction barrier diode designs such as "W-SL" [11], CBIRD [12], and the so called "M-barrier" [1,13,14].

In this work we study the performance of two structures with bandgap close to 0.25 eV, corresponding to 5.0 μm wavelength. One, structure "A", is a conventional homojunction diode design, whereas the other, structure "B", is an abrupt heterojunction *p–i–n* diode where the *i*- and *n*-type regions have larger bandgap, aligned to form a barrier in the valence band that block majority carriers from the *p*-type absorber. This design is in many respects similar to that of Refs. [1] and [14].

2. Experimental

Structures A and B were both grown on *n*-type (Te-doped) GaSb (100) substrates using solid source molecular beam epitaxy (MBE).

Structure A was grown using a V-80H VG Semicon system, which was equipped with a valve cracker source for arsenic a uni-

* Corresponding author. Tel.: +46 8 793 66 03; fax: +46 8 750 54 30.
E-mail address: Carl.Asplund@ir-nova.se (C. Asplund).

1350-4495/$ - see front matter © 2013 Elsevier B.V. All rights reserved.
http://dx.doi.org/10.1016/j.infrared.2012.12.004

valve cracker source for Sb, and SUMO® cells for the group III (Ga/In) fluxes. All superlattice (SL) periods consists of 10 monolayers (ML) InAs/10 ML GaSb, with various levels of doping. The growth sequence is, from bottom and up, a 0.9 μm thick Si-doped *n*-contact SL, a 2.1 μm non-intentionally doped *p*-type SL absorber, and 0.4 μm thick Be-doped *p*-type SL, followed by a 0.16 μm GaSb *p*-type contact layer. The doping concentration of the Be and Si-doped layers is $\sim 4 \times 10^{18}$ cm^{-3}.

Structure B consists of a 0.3 μm lattice matched $InAs_{0.09}Sb_{0.91}$ etch-stop layer, followed by 0.7 μm heavily Si-doped *n*-type "M-superlattice" (M-SL) bottom contact, 0.5 μm lightly doped *n*-type M-SL, 3 μm weakly doped *p*-type SL absorber, 0.1 μm of an intermediate bandgap heavily Be-doped *p*-type SL, and finally a 0.1 μm thick heavily Be-doped *p*-type GaSb contact layer. The M-SL periods consist of InAs/GaSb/AlSb/GaSb in the proportions 10/1/4/1 ML, whereas the absorber SL consists of 9.5 ML InAs/11.5 ML GaSb. The top and bottom contacts are doped to 2×10^{18} and 6×10^{17} cm^{-3}, respectively, whereas the doping concentration in the absorber is 1×10^{16} cm^{-3} (*p*-type).

Photoluminescence (PL) spectra were taken at 77 K with a lock-in amplifier, using chopped 532 nm laser excitation and a Fourier transform infrared (FTIR) spectrometer in step-scan mode.

Standard III/V-processing was used to produce a detector array with 320 × 256 pixels and a pixel pitch of 30 μm from structure A; mesas were formed using a combination of dry and wet etching [6], after which they were passivated using polymer based passivation. Mirror and contact metal was evaporated and after dicing the detector material was hybridized to an ISC9705 readout. Finally, the substrate was fully removed. A fill factor of 90% was achieved using this process.

Structure B was processed in a similar fashion, but into a 640 × 512 pixel array with 15 μm pitch. To study the dark currents for this structure single pixel detectors of different sizes were also produced using the same process as described above, except the substrate was not removed. The optical loss in the substrate was estimated to be 25%. All results reported in this paper were obtained for devices without antireflection (AR) coating.

The quantum efficiency (QE) spectrum was measured using a dispersive spectrometer with a calibrated photon flux entering through the substrate, or – in the case of removed substrate – through the bottom contact material. A lock-in amplifier was used to suppress noise and background signal.

An 8 × 8 band $k \cdot P$ transfer-matrix envelope function approximation simulator was used to model electron band structure and envelope functions for superlattices with arbitrary number of layers per period [15,16]. Material data, including band offsets were taken from Ref. [18]. Fractions of an InSb monolayer were added at the interfaces to obtain an average lattice match in each period, just as in MBE growth.

3. Results and discussion

3.1. Homojunction diode results, structure A

Using the nominal thicknesses described above the $k \cdot P$ model predicted a bandgap around 5.4 μm for structure A. Before processing of the wafer, a 77 K photoluminescence peak was observed at 4.9 μm. After hybridization of a part of a processed FPA to a fan-out circuit and subsequent removal of the substrate, the external quantum efficiency at 100–120 K was measured to be around 40%, with the 10% cutoff $\lambda_{co,10\%}$ at 5.2 μm; see Fig. 1. We therefore conclude that the model works rather well. The variation of the efficiency with temperature is modest – less than 20% in the operating temperature interval from 40 to 120 K. As expected for a homojunction device, the efficiency is not dependent on the applied voltage: there is no significant change in QE when the bias is increased from 0 V.

The dark current was measured in the same setup, with the addition of a cold shield. The dark current is dominated by Shockley–Read–Hall (SRH) generation in the space charge region for operating temperatures around 100 K, but becomes increasingly diffusion-like as the temperature is further increased. Fig. 2 shows an attempt to fit the dark current to a model similar to that of Gilmore et al. [17]. In the 110–140 K interval, the so extracted diffusion current contribution has an activation energy E_a of 0.20 eV, while that of the space charge SRH component is lower, 0.14 eV. The overall tendency for the activation energy of the total dark current is to increase with increasing temperature; see Fig. 3. At −0.05 V bias the dark current of structure A is 3×10^{-7} A/cm^2 at 80 K, 2×10^{-5} A/cm^2 at 100 K, and 4×10^{-4} A/cm^2 at 120 K, which is reasonably good for a homojunction structure with 5 μm cutoff processed into 30 × 30 μm^2 mesas [19,20].

For the optimum level of the SRH trap, the intrinsic level, the depletion current becomes $J_{dep} = qn_iW/(\tau_{n0} + \tau_{p0})$, where the n_i is

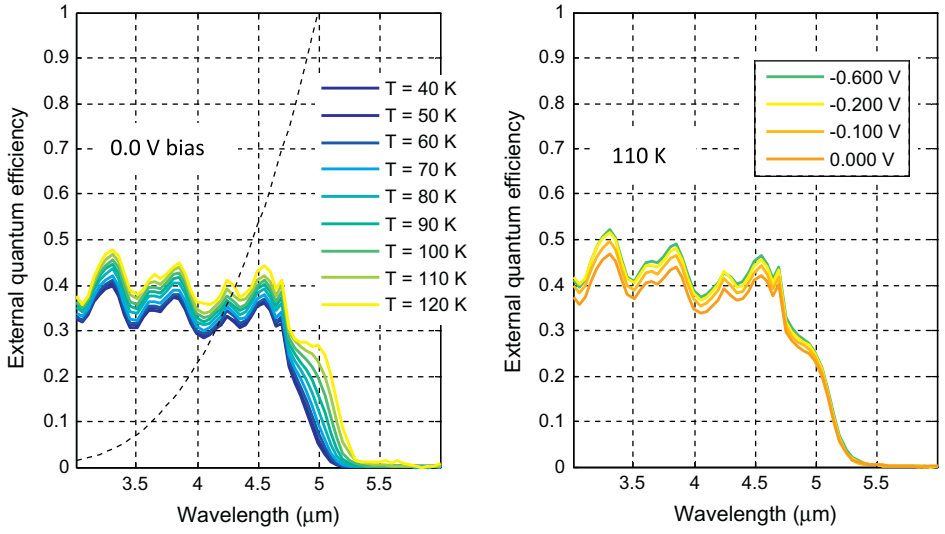

Fig. 1. Measured external quantum efficiency of the homojunction diode, structure A, using backside illumination. The 8 × 8 and 30 × 30 μm^2 pixels were hybridized to a fan-out circuit and the substrate was completely removed. The 50% cutoff and 10% cutoff occur at 5.0 and 5.2 μm, respectively, for 110 K operating temperature.